

# Spectroscopy of Very Heavy Elements

Paul Greenlees

Department of Physics  
University of Jyväskylä

École Joliot Curie  
30.9.-05.10.2012  
Fréjus, France



# What is the link?



# Outline

- 1 Introduction
- 2 Experimental Approaches
- 3 Alpha Decay (Fine Structure) Spectroscopy
- 4 In-Beam Spectroscopy
- 5 Structure of High-K States
- 6 Future Perspectives

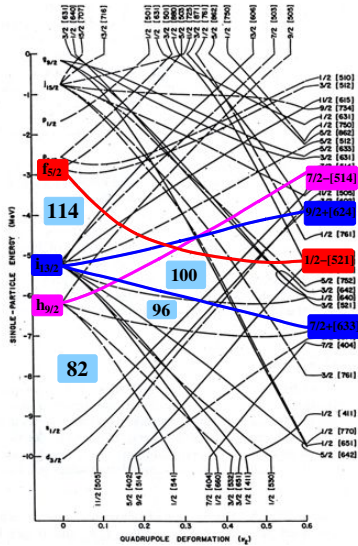
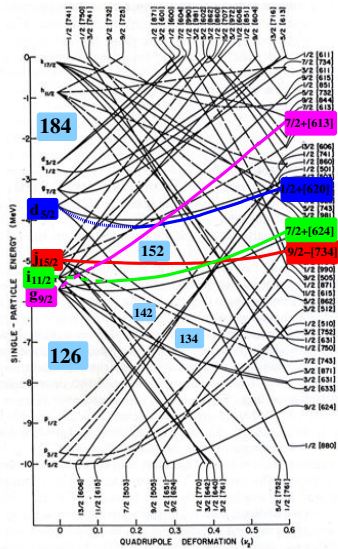


# Outline

- 1 Introduction
- 2 Experimental Approaches
- 3 Alpha Decay (Fine Structure) Spectroscopy
- 4 In-Beam Spectroscopy
- 5 Structure of High-K States
- 6 Future Perspectives



# What is the structure of SHE?



# Outline

- 1 Introduction
- 2 Experimental Approaches
- 3 Alpha Decay (Fine Structure) Spectroscopy
- 4 In-Beam Spectroscopy
- 5 Structure of High-K States
- 6 Future Perspectives

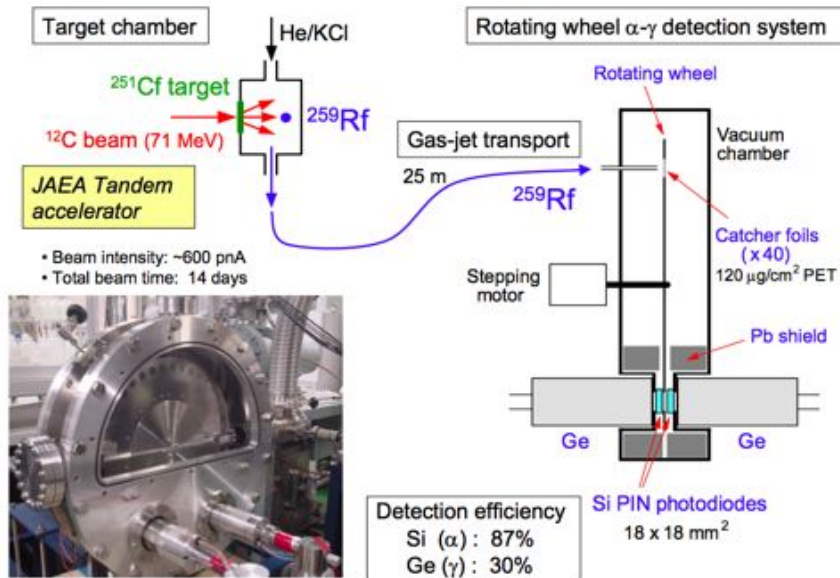


# Outline

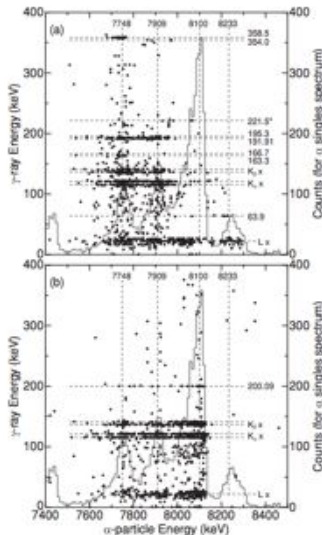
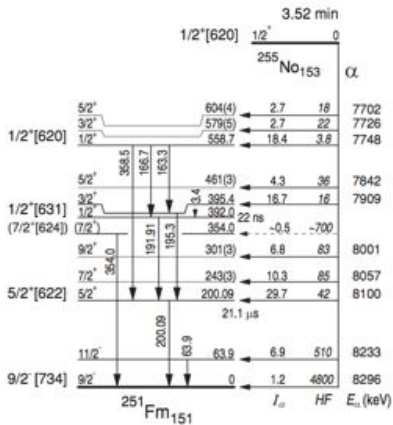
- 1 Introduction
- 2 Experimental Approaches
- 3 Alpha Decay (Fine Structure) Spectroscopy
- 4 In-Beam Spectroscopy
- 5 Structure of High-K States
- 6 Future Perspectives



# Decay Spectroscopy - Case Study $^{255}\text{No}$



# Decay Spectroscopy - Case Study $^{255}\text{No}$



M.Asai et al., PRC **83**, 014315 (2011) and ARIS2011

# Decay Spectroscopy - Case Study $^{255}\text{No}$

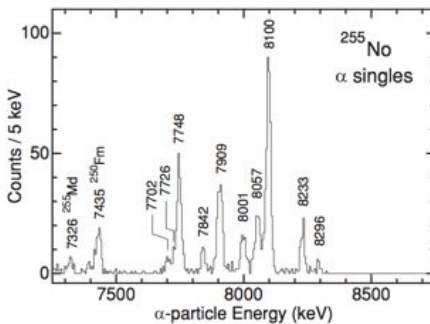
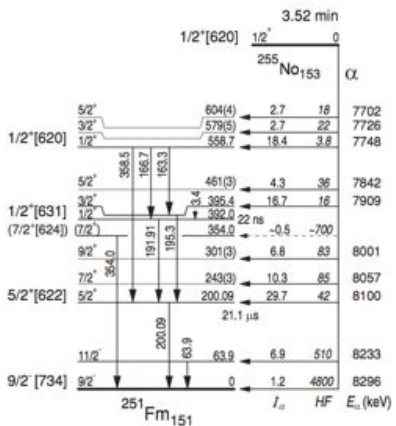


FIG. 6.  $\alpha$  fine-structure spectrum of  $^{255}\text{No}$  measured during the period of 90–360 s after the ends of the source depositions.

M.Asai et al., PRC **83**, 014315 (2011) and  
ARIS2011

# Decay Spectroscopy - Case Study $^{255}\text{No}$

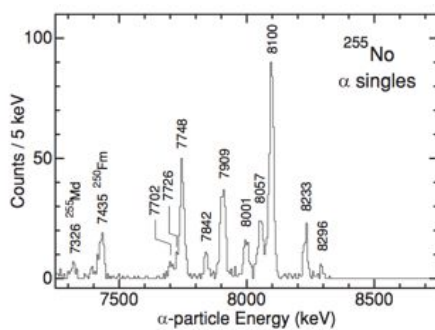
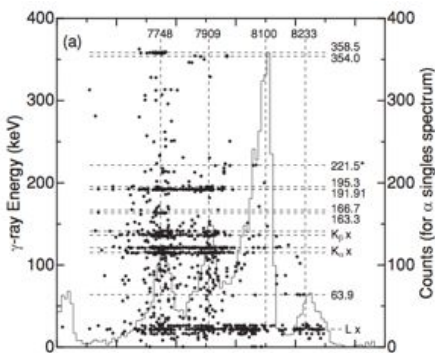


FIG. 6.  $\alpha$  fine-structure spectrum of  $^{255}\text{No}$  measured during the period of 90–360 s after the ends of the source depositions.

# Decay Spectroscopy - Case Study $^{255}\text{No}$

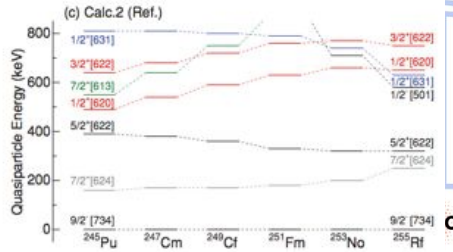
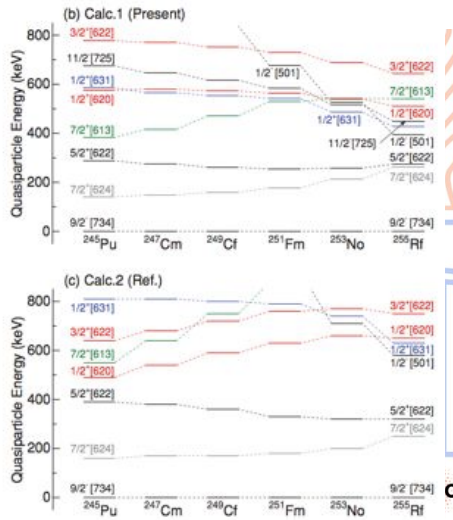
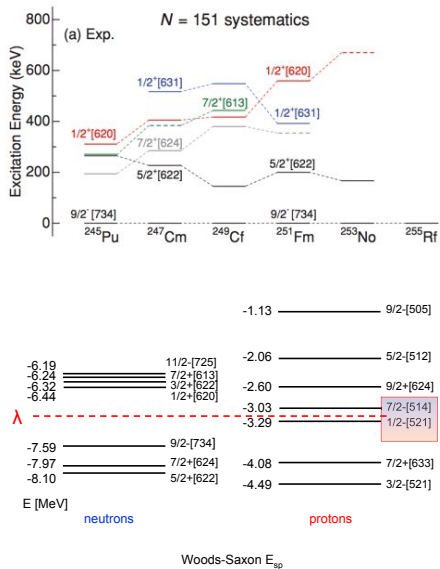
TABLE III. Hindrance factors of  $\alpha$  transitions from the  $1/2^+[620]$  ground states in the  $N = 153$  isotones  $^{251}\text{Cf}$ ,  $^{253}\text{Fm}$ , and  $^{255}\text{No}$  to excited states in the  $N = 151$  daughters. They were calculated on the basis of the Preston's spin-independent theory [21] using the radius parameters given in Refs. [22,23].

Nilsson orbital	Populated level	Hindrance factor		
		$^{251}\text{Cf} \rightarrow ^{247}\text{Cm}$	$^{253}\text{Fm} \rightarrow ^{249}\text{Cf}$	$^{255}\text{No} \rightarrow ^{251}\text{Fm}$
$1/2^+[620]$	$5/2^+$	11	17	18
	$3/2^+$	19	23	22
	$1/2^+$	2.6	3.0	3.8
$1/2^+[631]$	$5/2^+$	32	31	36
	$3/2^+$	11	11	16
$5/2^+[622]$	$9/2^+$	77	48	83
	$7/2^+$	134	72	85
	$5/2^+$	31	25	42
$9/2^-[734]$	$11/2^-$	512	350	510
	$9/2^-$	\$100	3200	4800

TABLE IV.  $B(E2)$  values of  $1/2^+[631] \rightarrow 5/2^+[622]$  and  $1/2^+[620] \rightarrow 5/2^+[622]$  transitions in various actinide nuclei.

Nuclide	$E_{\text{level}}$ (keV)	$t_{1/2}$	$E_{\gamma}$ (keV)	$B(E2)$ (W.u.)
$1/2^+[631] \rightarrow 5/2^+[622]$				
$^{239}\text{U}_{147}$	133.7	0.78(4) $\mu\text{s}$	133.7	0.0404(21)
$^{241}\text{Pu}_{147}$	161.4	0.88(5) $\mu\text{s}$	161.4	0.0218(12)
$^{243}\text{Cm}_{147}$	87.4	1.08(3) $\mu\text{s}$	87.4	0.0313(9)
$^{243}\text{Pu}_{149}$	383.6	0.33(3) $\mu\text{s}$	96.2	0.114(10)
$^{245}\text{Cm}_{149}$	355.9	0.29(2) $\mu\text{s}$	103.0	0.105(7)
$^{251}\text{Fm}_{151}$	392.0	22(3) ns	191.9	0.41(6)
$1/2^+[620] \rightarrow 5/2^+[622]$				
$^{243}\text{Pu}_{151}$	311	0.33(2) $\mu\text{s}$	47	0.139(8)
$^{247}\text{Cm}_{151}$	404.9	100.6(6) ns	177.5	0.1338(8)

# Decay Spectroscopy - Case Study $^{255}\text{No}$



# Decay spectroscopy of $^{255}\text{Lr}$

A.Chatillon et al., EPJA **30** 397 (2006)

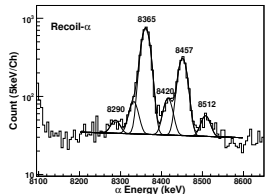


Fig. 4. Portion of the  $\alpha$ -decay spectrum, resulting from recoil- $\alpha$  correlations, in the  $^{255}\text{Lr}$  region. Data are taken from the JYFL experiment.

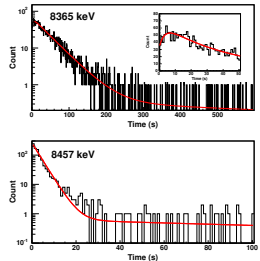


Fig. 5. Decay curves corresponding to the 8365 keV (upper panel) and 8457 keV (lower panel)  $\alpha$ -decay lines.

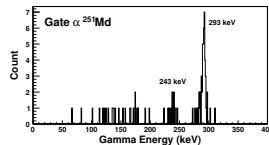


Fig. 9. Upper panel: matrix corresponding to prompt  $\alpha$ - $\gamma$  correlations. Lower panel:  $\gamma$  transition in coincidence with the  $^{251}\text{Md}$   $\alpha$  line. Data are taken from the GANIL experiment.

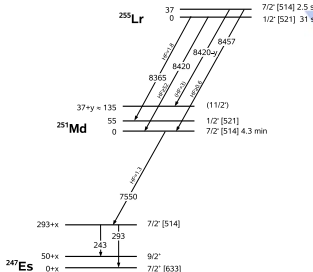
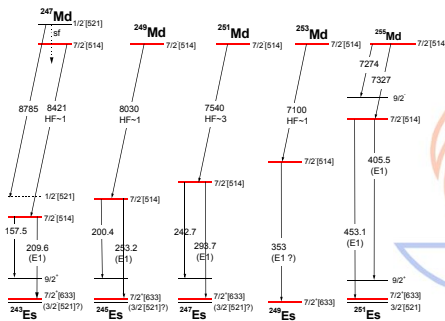
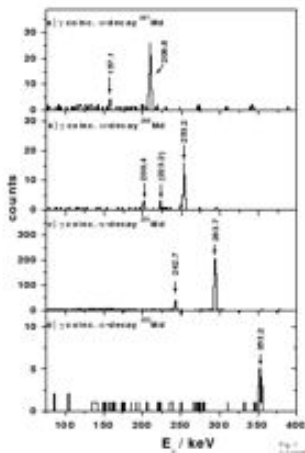


Fig. 13. Level scheme of  $^{247}\text{Es}$ ,  $^{251}\text{Md}$  and  $^{255}\text{Lr}$  deduced from experimental data. The tentative 8290 keV line from  $^{255}\text{Lr}$  is not shown.

# Decay spectroscopy at SHIP

Courtesy of F.P.Heßberger



- Trace separation of states from 4 spherical shells:
- $\pi[521]1/2^-$  ( $2f_{5/2}$ )
- $\pi[514]7/2^-$  ( $1h_{9/2}$ )
- $\pi[633]7/2^+$  ( $1i_{13/2}$ )
- $\pi[521]3/2^-$  ( $2f_{7/2}$ )

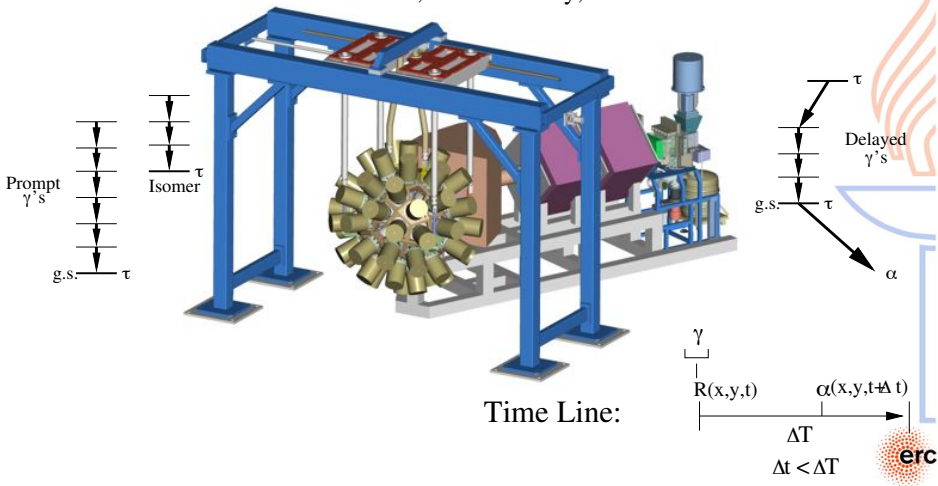
# Outline

- 1 Introduction
- 2 Experimental Approaches
- 3 Alpha Decay (Fine Structure) Spectroscopy
- 4 In-Beam Spectroscopy
- 5 Structure of High-K States
- 6 Future Perspectives



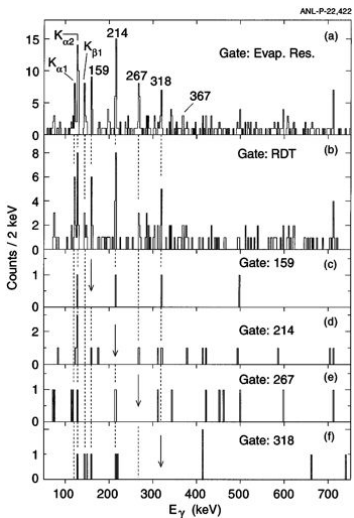
# Principles of Recoil-Decay Tagging

## Tagging Techniques Recoil, Recoil-Decay, Isomer



# Over a decade of in-beam studies in the region of $^{254}\text{No}$

P.Reiter et al., PRL **82**, 509 (1999)



VOLUME 82, NUMBER 3

PHYSICAL REVIEW LETTERS

18 JANUARY 1999

## Ground-State Band and Deformation of the $Z = 12$ Isotope $^{254}\text{No}$

P. Reiter,<sup>1</sup> T.L. Khoo,<sup>1</sup> C.J. Lister,<sup>1</sup> D. Seweryniak,<sup>2</sup> I. Ahmad,<sup>1</sup> M. Alcorta,<sup>3</sup> M.P. Carpenter,<sup>1</sup> J.A. Cizewski,<sup>1,3</sup> C.N. Davids,<sup>1</sup> G. Gervais,<sup>1</sup> J.P. Greene,<sup>1</sup> J.W.F. Hennig,<sup>1</sup> R.V.F. Janssens,<sup>1</sup> T. Lauritsen,<sup>1</sup> S. Siem,<sup>1,8</sup> A.A. Sonzogni,<sup>1</sup> D. Sullivan,<sup>1</sup> J. Uustala,<sup>1</sup> I. Wiedenhofer,<sup>1</sup> N. Amati,<sup>2</sup> P.A. Butler,<sup>1</sup> A.J. Chesser,<sup>1</sup> K.Y. Ding,<sup>2</sup> N. Fotiades,<sup>2</sup> J.D. Fox,<sup>8</sup> P.T. Greenlees,<sup>2</sup> R.-D. Herzberg,<sup>2</sup> G.D. Jones,<sup>7</sup> W. Kotorn,<sup>2</sup> M. Leino,<sup>8</sup> and K. Vetter<sup>2</sup>

<sup>1</sup>Argonne National Laboratory, Argonne, Illinois 60439

<sup>2</sup>University of Liverpool, Liverpool L69 7ZE, England

<sup>3</sup>Florida Institute of Technology, Melbourne, Florida 32903

<sup>4</sup>Florida State University, Tallahassee, Florida 32306

<sup>5</sup>DAPNIA/SP2N, CEA Saclay, F-91191 Gif-sur-Yvette Cedex, France

<sup>6</sup>University of Jyväskylä, Jyväskylä, Finland

<sup>7</sup>Lawrence Berkeley National Laboratory, Berkeley, California 94720

<sup>8</sup>University of Oslo, Oslo, Norway

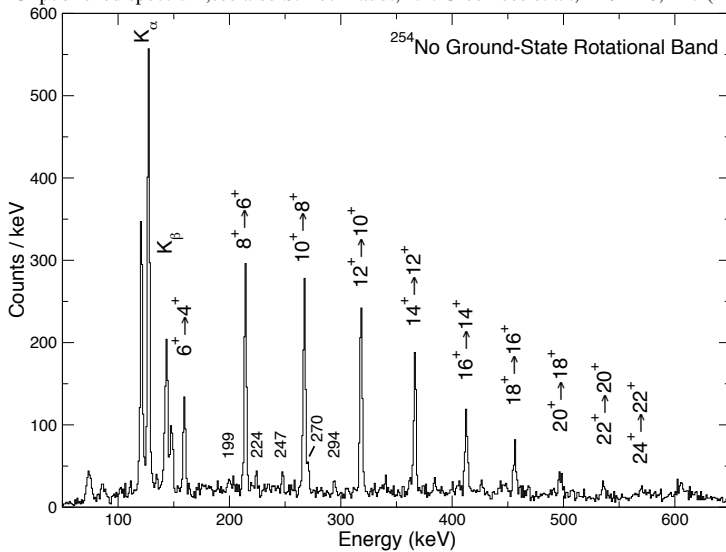
(Received 21 October 1998)

The ground-state band of the  $Z = 12$  isotope  $^{254}\text{No}$  has been identified up to spin 14, indicating that the nucleus is deformed. The oblate ground-state deformation,  $\beta = -0.27$ , is in agreement with theoretical predictions. These observations confirm that the shell-correction energy responsible for the stability of transneptunium nuclei is partly derived from deformation. The survival of  $^{254}\text{No}$  up to spin 14 means that its fission barrier persists at least up to that spin. [S0031-9007(98)08223-4]



# In-beam $\gamma$ -ray Spectroscopy of $^{254}\text{No}$

Unpublished spectrum, see also S. Eeckhaudt, P.T. Greenlees et al., EPJA **26**, 227 (2005)



# Rotational Bands

$(18^+)$   $(2372)$   
 $(18^+)$   $(2280)$

$(16^+)$   $(1921)$   
 $(16^+)$   $(1845)$

$(14^+)$   $(1508)$   
 $(14^+)$   $(1448)$

$(12^+)$   $(1137)$   
 $(12^+)$   $(1091)$

$(10^+)$   $(813)$   
 $(10^+)$   $(779)$

$(8^+)$   $(539)$   
 $(8^+)$   $(516)$

$(6^+)$   $(317)$   
 $(6^+)$   $(304)$

$(4^+)$   $(152)$   
 $(2^+)$   $(46)$

$0^-$   
 $248\text{ Fm}$

$(18^+)$   $(2395)$   
 $(18^+)$   $(2339)$

$(16^+)$   $(1942)$   
 $(16^+)$   $(1883)$

$(14^+)$   $(1525)$   
 $(14^+)$   $(1470)$

$(12^+)$   $(1150)$   
 $(12^+)$   $(1104)$

$(10^+)$   $(822)$   
 $(10^+)$   $(786)$

$(8^+)$   $(545)$   
 $(8^+)$   $(513)$

$(6^+)$   $(321)$   
 $(6^+)$   $(305)$

$(4^+)$   $(154)$   
 $(2^+)$   $(48)$

$0^-$   
 $250\text{ Fm}$

$0^-$   
 $252\text{ No}$

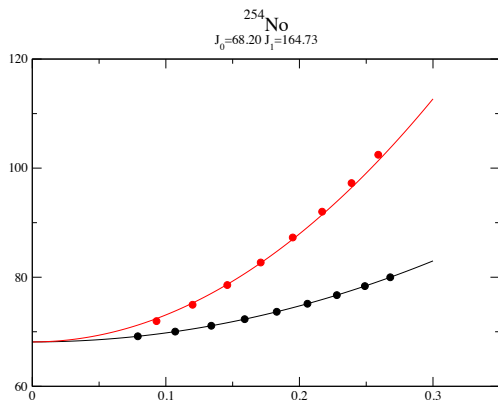
$0^-$   
 $254\text{ No}$

## Harris Fits

- $\mathcal{J}^{(1)} = \hbar^2 \frac{2I-1}{E_{\gamma 1}}$
- $\mathcal{J}^{(2)} = \frac{4\hbar^2}{\Delta E_\gamma}$
- $\mathcal{J}^{(1)} = \mathcal{J}_0 + \mathcal{J}_1 \omega^2$
- $\mathcal{J}^{(2)} = \mathcal{J}_0 + 3\mathcal{J}_1 \omega^2$
- $I = \mathcal{J}_0 \omega + \mathcal{J}_1 \omega^3 + 1/2$



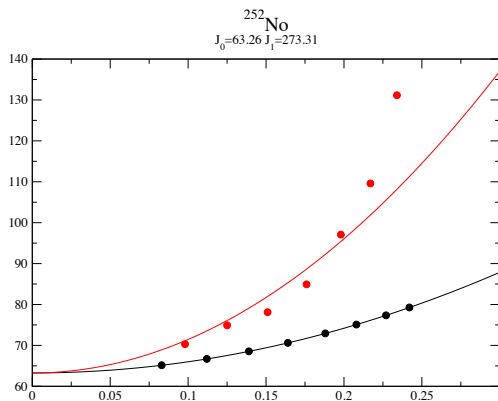
# Rotational Bands



## Harris Fits

- $\mathcal{J}^{(1)} = \hbar^2 \frac{2I-1}{E_{\gamma 1}}$
- $\mathcal{J}^{(2)} = \frac{4\hbar^2}{\Delta E_\gamma}$
- $\mathcal{J}^{(1)} = \mathcal{J}_0 + \mathcal{J}_1 \omega^2$
- $\mathcal{J}^{(2)} = \mathcal{J}_0 + 3\mathcal{J}_1 \omega^2$
- $I = \mathcal{J}_0 \omega + \mathcal{J}_1 \omega^3 + 1/2$

# Rotational Bands

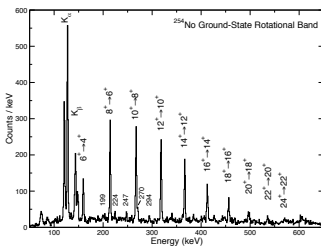


## Harris Fits

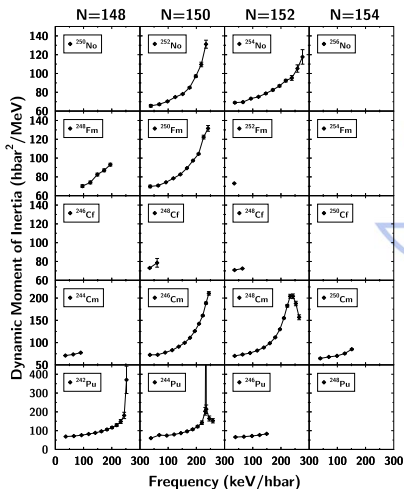
- $\mathcal{J}^{(1)} = \hbar^2 \frac{2I-1}{E_{\gamma 1}}$
- $\mathcal{J}^{(2)} = \frac{4\hbar^2}{\Delta E_\gamma}$
- $\mathcal{J}^{(1)} = \mathcal{J}_0 + \mathcal{J}_1 \omega^2$
- $\mathcal{J}^{(2)} = \mathcal{J}_0 + 3\mathcal{J}_1 \omega^2$
- $I = \mathcal{J}_0 \omega + \mathcal{J}_1 \omega^3 + 1/2$

# In-beam studies in region of $^{254}\text{No}$

S. Eeckhaudt, P.T. Greenlees et al., EPJA **26**, 227 (2005)



- Confirmed deformed nature of nuclei around  $^{254}\text{No}$
- Showed fission barrier robust with spin ( $> 20\hbar$ )
- Faster alignment at  $N=150$  compared to  $N=152$  ( $\pi i_{13/2}, \nu j_{15/2}$ )
- Excellent testing ground for theory; e.g.  
Duguet et al., NPA **679**, 427 (2001),  
Bender et al., NPA **723**, 354 (2003).  
Afanasjev et al., PRC **67**, 024309 (2003),  
Egido and Robledo, PRL **85** 1198 (2000)

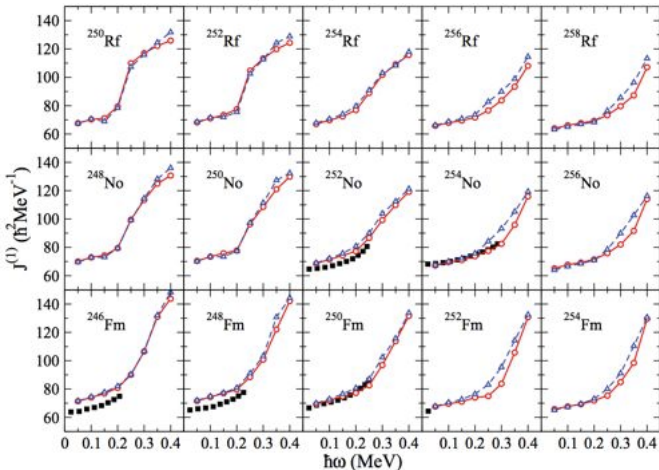


# Theory - $N=150$ vs. $N=152$

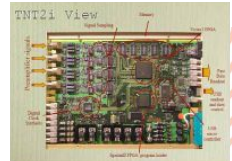
PHYSICAL REVIEW C 86, 011301(R) (2012)

## Understanding the different rotational behaviors of $^{252}\text{No}$ and $^{254}\text{No}$

H. L. Liu,<sup>1,\*</sup> F. R. Xu,<sup>2</sup> and P. M. Walker<sup>3,4</sup>



# Recent history of JUROGAM



- Fifth and final campaign ended May 2008
- 2003 - 2008: 67 experiments, 11000 hours beam on target
- 2008: Fully instrumented with TNT2 digital electronics
- TNT2 cards in collaboration with CNRS/IN2P3 GABRIELA
- Superseded by JUROGAM II

PRL 102, 212501 (2009)

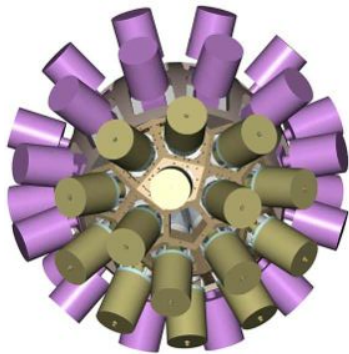
PHYSICAL REVIEW LETTERS

week ending  
29 MAY 2009

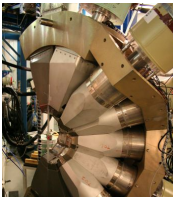
## $\gamma$ -Ray Spectroscopy at the Limits: First Observation of Rotational Bands in $^{255}\text{Fr}$

S. Ketelbant,<sup>1,\*</sup> P.T. Greenlees,<sup>1</sup> D. Ackermann,<sup>2</sup> S. Antalic,<sup>3</sup> E. Clément,<sup>4</sup> I.G. Darby,<sup>5,7</sup> O. Dorvaux,<sup>6</sup> A. Drouart,<sup>4</sup> S. Eckehaus,<sup>4</sup> B.J.P. Gall,<sup>6</sup> A. Görgen,<sup>3</sup> T. Grahn,<sup>1,2</sup> C. Gray-Jones,<sup>5</sup> K. Hauschild,<sup>7</sup> R.-D. Herzberg,<sup>3</sup> F.P. Heßberger,<sup>2</sup> U. Jakobsson,<sup>5</sup> G.D. Jones,<sup>7</sup> P. Jones,<sup>1</sup> R. Julin,<sup>1</sup> S. Juttilainen,<sup>1</sup> T.-L. Khoa,<sup>8</sup> W. Korten,<sup>3</sup> M. Leino,<sup>1</sup> A.-P. Leppänen,<sup>1,8</sup> J. Ljungvall,<sup>5</sup> S. Moon,<sup>2</sup> M. Nyman,<sup>1</sup> A. Oberstedt,<sup>4</sup> J. Pakarinen,<sup>1,2</sup> E. Pan,<sup>2</sup> P. Papadakis,<sup>5</sup> P. Peura,<sup>1</sup> J. Piot,<sup>6</sup> A. Prichard,<sup>5</sup> P. Rahkila,<sup>1</sup> D. Rostron,<sup>7</sup> P. Ruotsalainen,<sup>1</sup> M. Sandzelius,<sup>9</sup> J. Särén,<sup>1</sup> C. Scholey,<sup>1</sup> J. Sorri,<sup>1</sup> A. Steer,<sup>10</sup> B. Sulignano,<sup>14</sup> Ch. Theisen,<sup>1</sup> J. Uusitalo,<sup>5</sup> M. Venhart,<sup>3,11</sup> M. Zielinska,<sup>11</sup> M. Bender,<sup>12,13</sup> and P.-H. Heenen<sup>14</sup>

# The JUROGAM II Germanium Array



- 24 Clover and 15 Tapered Ge detectors - GAMMAPOOL resource
- Total Photopeak Efficiency  $\simeq 6\%$  @ 1.3 MeV
- Excellent  $\gamma$ - $\gamma$  efficiency
- Autofill system built by University of York, part of GREAT
- Instrumented with TNT2 / Lyrtech digital electronics
- Higher counting rates, higher beam intensities
- 20,000 hours in-beam  $\gamma$ -ray spectroscopy passed in 2011



Paul Greenlees (JYFL, Finland)



Spectroscopy of VHE

PHYSICAL REVIEW C 85, 041301(R) (2012)  
RAPID COMMUNICATIONS

**In-beam spectroscopy with intense ion beams: Evidence for a rotational structure in  $^{246}\text{Fm}$**

J. Piot,<sup>1,\*</sup> B. J.-P. Gall,<sup>1</sup> O. Dorvaux,<sup>1</sup> P. T. Greenlees,<sup>2</sup> N. Rowley,<sup>3</sup> L. L. Andersson,<sup>4</sup> D. M. Cox,<sup>4</sup> F. Dechery,<sup>5</sup> T. Grahn,<sup>2</sup> K. Hauschild,<sup>2,6</sup> G. Henning,<sup>8,2</sup> A. Herzan,<sup>2</sup> R.-D. Herzberg,<sup>7</sup> F. P. Heßberger,<sup>8</sup> U. Jakobsson,<sup>2</sup> P. Jones,<sup>2,7</sup> R. Julin,<sup>2</sup> S. Juutinen,<sup>2</sup> S. Ketelbaut,<sup>2</sup> T.-L. Khoo,<sup>9</sup> M. Leino,<sup>2</sup> J. Ljungvall,<sup>6</sup> A. Lopez-Martens,<sup>2,10</sup> P. Nieminen,<sup>2</sup> J. Pakarinen,<sup>8,11</sup> P. Papadakis,<sup>8</sup> E. Paré,<sup>2</sup> P. Peura,<sup>2</sup> P. Rakhlin,<sup>2</sup> S. Rinta-Antila,<sup>2</sup> J. Rubert,<sup>1</sup> P. Ruotsalainen,<sup>2</sup> M. Sandzelius,<sup>2</sup> J. Särén,<sup>2</sup> C. Scholey,<sup>2</sup> D. Seweryniak,<sup>7</sup> J. Sorri,<sup>2</sup> B. Sulignano,<sup>2</sup> and J. Uusitalo<sup>2</sup>



# Next step - push to Rutherfordium Z=104

- Can produce  $^{256}\text{Rf}$  using:  
 $^{50}\text{Ti} + ^{208}\text{Pb} \rightarrow ^{256}\text{Rf} + 2\text{n}$
- Cross section below 20 nb
- Need high intensity  $^{50}\text{Ti}$  beam
- Used up to 70 pnA in  $^{246}\text{Fm}$  experiment
- Rotating target wheel built at IPHC Strasbourg

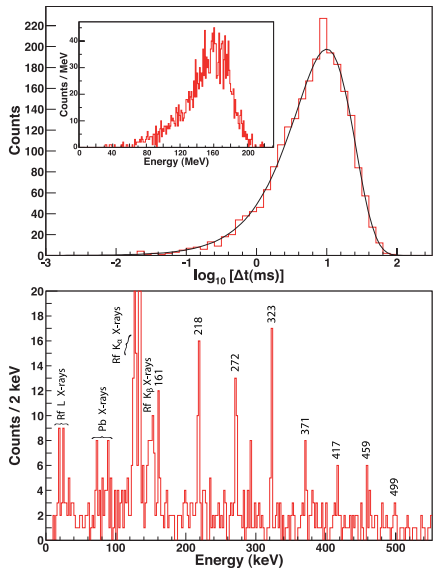


## $^{50}\text{Ti}$ MIVOC beam development

- Metallic Ions from VOolatile Compounds
- Method developed at JYFL
- Synthesis of enriched  $^{50}\text{Ti}$  compound led by IPHC Strasbourg
- Several years of hard work!
- 19  $\mu\text{A}$  of  $^{50}\text{Ti}^{11+}$  from ECR
- 490 enA on target
- Low consumption - 0.2 mg/hr
- See J.Rubert et al., NIMB **276**, 33 (2012)



# In-beam spectroscopy of SHE: $^{256}\text{Rf}$



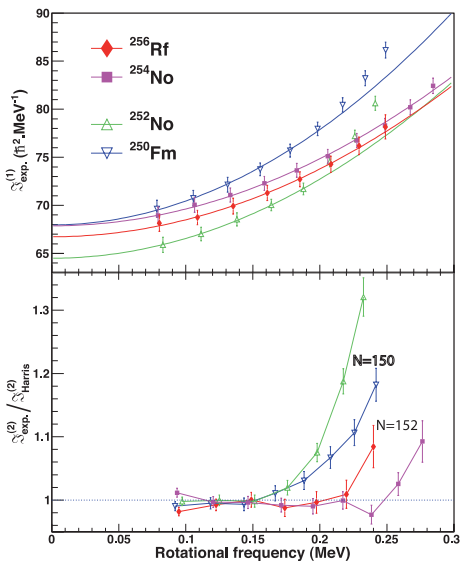
## Experimental Details

- $^{50}\text{Ti} + ^{208}\text{Pb} \Rightarrow ^{256}\text{Rf} + 2\text{n}$
- JUROGAM II, RITU, GREAT
- Enriched  $^{50}\text{Ti}$  beam from MIVOC
- 450 hours, 29pnA beam, 2210 observed fissions
- Cross section 17 nb

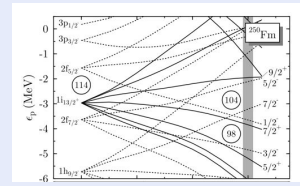
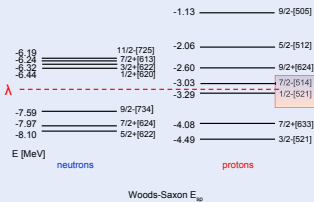
P.T.Greenlees, J.Rubert et al.,  
PRL **109**, 012501 (2012)



# In-beam spectroscopy of SHE: $^{256}\text{Rf}$

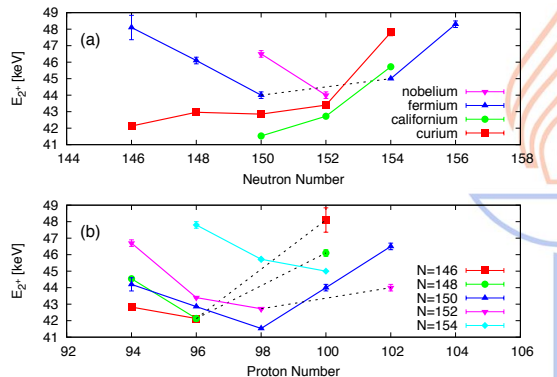
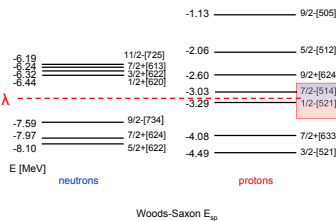


## Single-particle energies



P.T.Greenlees, J.Rubert et al.,  
PRL 109, 012501 (2012)

# Experimental $2^+$ Energies

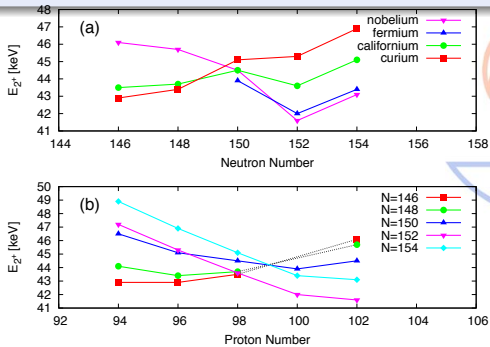
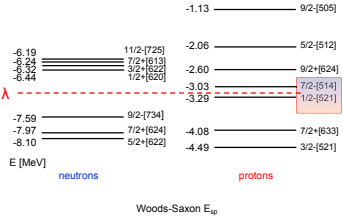


## Harris Fits

- $\mathcal{J}^{(1)} = \hbar^2 \frac{2I-1}{E_{\gamma 1}}$
- $\mathcal{J}^{(2)} = \frac{4\hbar^2}{\Delta E_\gamma}$
- $\mathcal{J}^{(1)} = \mathcal{J}_0 + \mathcal{J}_1 \omega^2$
- $\mathcal{J}^{(2)} = \mathcal{J}_0 + 3\mathcal{J}_1 \omega^2$
- $I = \mathcal{J}_0 \omega + \mathcal{J}_1 \omega^3 + 1/2$

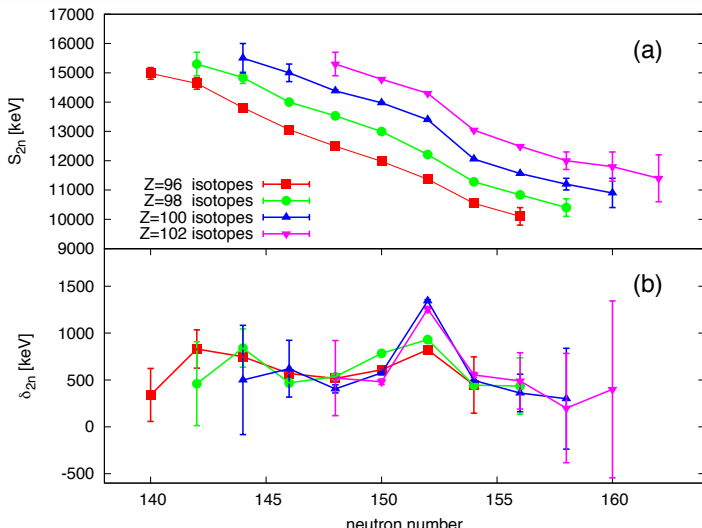
# Theoretical $2^+$ Energies

Sobiczewski, Muntian, Patyk. PRC **63**, 034306 (2001)



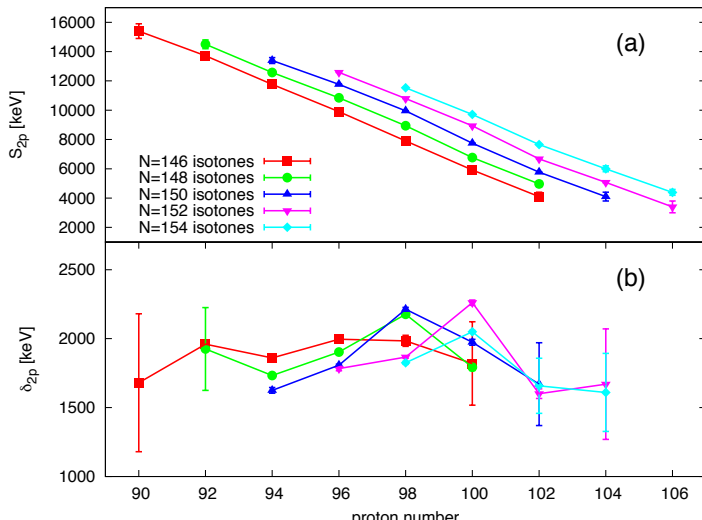
# Correlation to Masses - Isotopes

AME2003:  $S_{2n}(Z, N) = B(Z, N) - B(Z, N - 2)$ ,  $\delta_{2n}(Z, N) = S_{2n}(Z, N) - S_{2n}(Z, N + 2)$



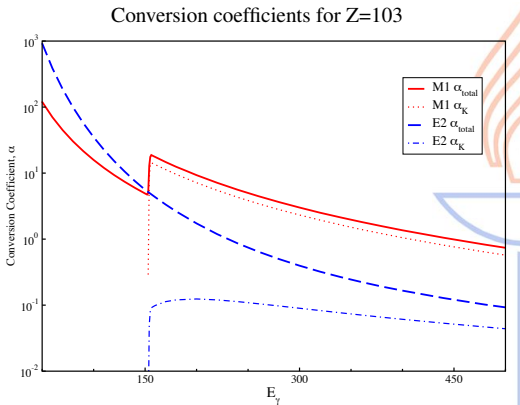
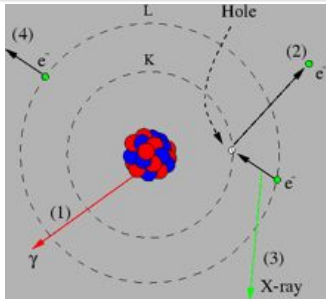
# Correlation to Masses - Isotones

AME2003:  $S_{2p}(Z, N) = B(Z, N) - B(Z - 2, N)$ ,  $\delta_{2p}(Z, N) = S_{2p}(Z, N) - S_{2p}(Z + 2, N)$



# Internal Conversion

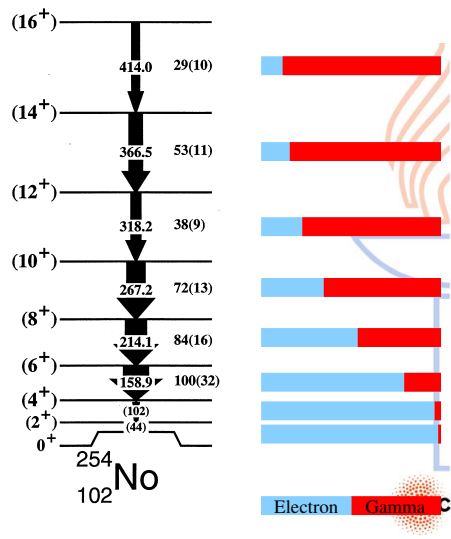
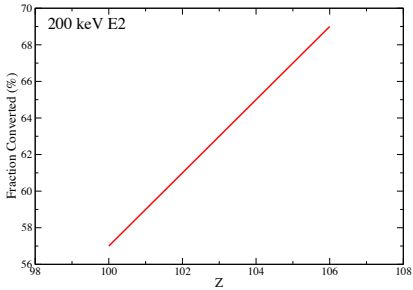
- $E_i = E_\gamma - B_i$ ;  
 $i = K, L_I, L_{II}, \dots, M_V, \dots$
- $\alpha_{tot} = \frac{N_e}{N_\gamma} = \alpha_K + \alpha_L + \dots$
- $\alpha \propto \frac{Z^3}{n^3 E_\gamma^{2.5}}$
- $\alpha$  increases strongly with multipolarity
- $\alpha$  larger for magnetic transitions



# Internal Conversion

Fraction of 200 keV E2 converted

$$f = \frac{\alpha}{1+\alpha}$$



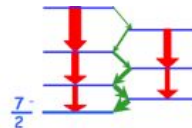
# Electromagnetic Properties

- Odd-proton orbitals in  $^{251}\text{Md}$
- $B(\text{M}1)/B(\text{E}2)$  depends on  $(g_K - g_R / Q_0)$

[514]  $\frac{7}{2}^+$

$g_K \sim 0.7$

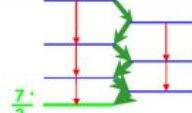
Mainly E2



[633]  $\frac{7}{2}^+$

$g_K \sim 1.3$

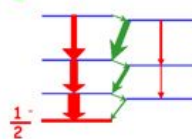
Mainly M1



[521]  $\frac{1}{2}^+$

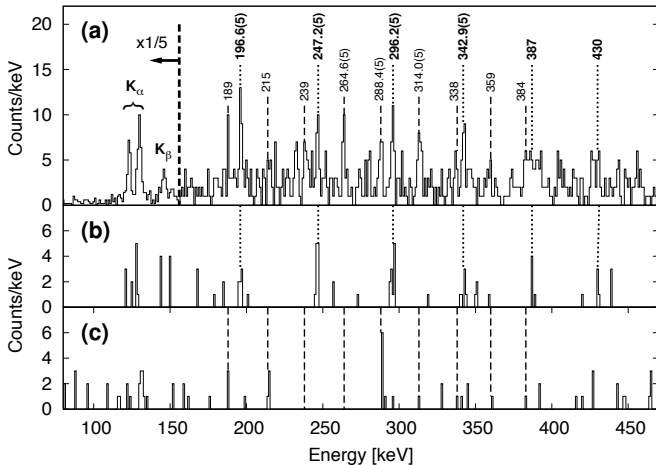
$a \sim 0.9:$   
 $g_K \sim -0.55$

Mainly E2



# In-beam $\gamma$ -ray Spectroscopy of $^{255}\text{Lr}$

$^{48}\text{Ca} + ^{209}\text{Bi} \Rightarrow ^{255}\text{Lr} + 2\text{n}$ ,  $\sigma \simeq 300 \text{ nb}$ , S. Ketelhut et al., PRL **102** 212501 (2009)



# Spectrometer Design Considerations

## Efficiency

Broad Range

Typically 0-1 MeV

Backscattering - normal incidence

## Magnetic Field

Profile

Strength

## Detector

Thickness

Size

Granularity

## Resolution

Intrinsic

Doppler Broadening

## Delta Electron Suppression

Kinematics

Biased Target

Physical Block

HV Barrier

High Counting Rate Capability

Tagging Techniques

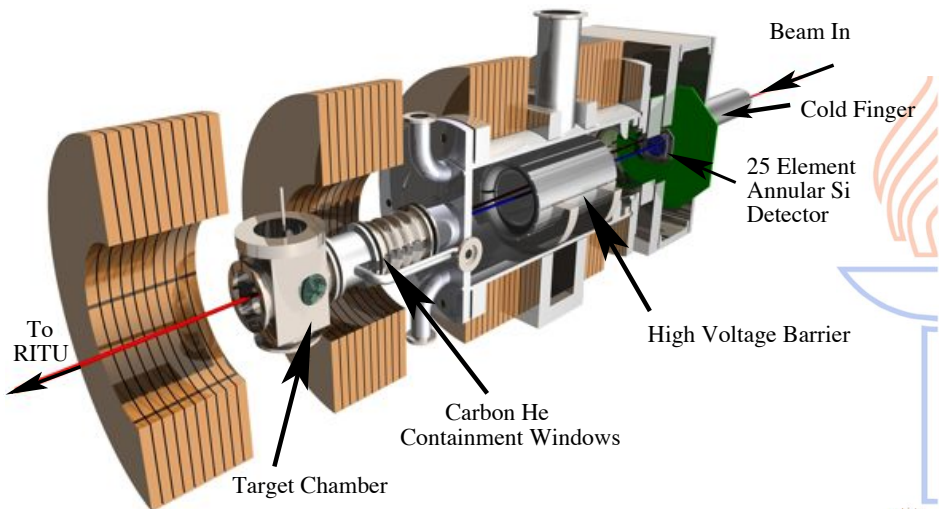
## Combination with Ge

Maintain Ge Efficiency

Maintain P/T

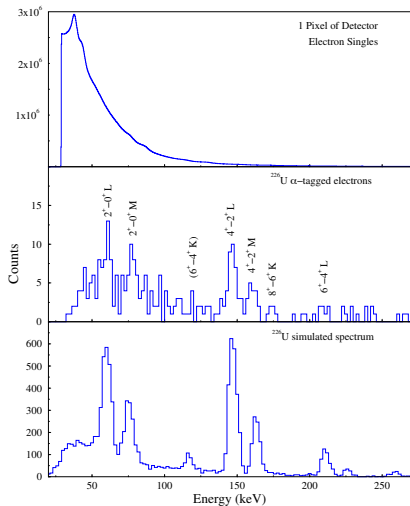
Effect of stray field

# The SACRED Electron Spectrometer



H. Kankaanpää et al., NIM A534, 503 (2004)  
P. A. Butler et al., NIM A381, 433 (1996)

# Recoil-Decay Tagging with SACRED



$\delta$  electrons produced with atomic cross sections!

H. Kankaanpää et al.,  
NIM A534, 503 (2004)  
see also:  
R.D. Humphreys et al.,  
PRC69, 064324 (2004)

# Conversion-Electron Spectroscopy of $^{254}\text{No}$

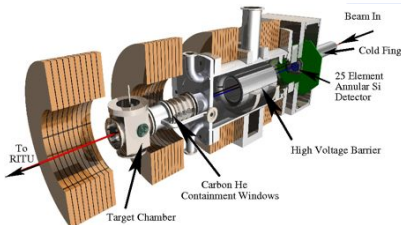
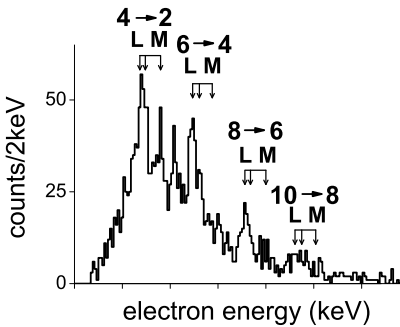
VOLUME 89, NUMBER 20

PHYSICAL REVIEW LETTERS

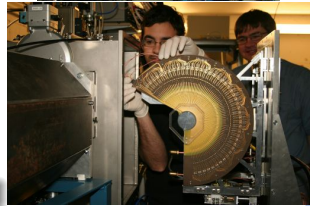
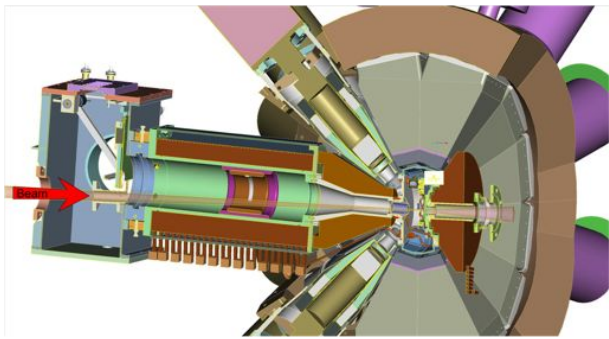
11 NOVEMBER 2002

## Conversion Electron Cascades in $^{254}\text{No}$

P. A. Butler,<sup>1</sup> R. D. Humphreys,<sup>1</sup> P. T. Greenlees,<sup>2</sup> R.-D. Herzberg,<sup>1</sup> D. G. Jenkins,<sup>1</sup> G. D. Jones,<sup>1</sup> H. Kankaanpää,<sup>2</sup> H. Kettunen,<sup>2</sup> P. Rahkila,<sup>2</sup> C. Scholey,<sup>1,2</sup> J. Uusitalo,<sup>2</sup> N. Amzal,<sup>1</sup> J. E. Bastin,<sup>1</sup> P. M. T. Brew,<sup>1</sup> K. Eskola,<sup>3</sup> J. Gerl,<sup>4</sup> N. J. Hammond,<sup>1</sup> K. Hauschild,<sup>5</sup> K. Helariutta,<sup>4</sup> F.-P. Heßberger,<sup>4</sup> A. Hürstel,<sup>5</sup> P. M. Jones,<sup>2</sup> R. Julin,<sup>2</sup> S. Juutinen,<sup>2</sup> A. Keenan,<sup>2</sup> T.-L. Khoo,<sup>6</sup> W. Korten,<sup>5</sup> P. Kuusiniemi,<sup>2</sup> Y. Le Coz,<sup>5</sup> M. Leino,<sup>2</sup> A.-P. Leppänen,<sup>2</sup> M. Muikku,<sup>2</sup> P. Nieminen,<sup>2</sup> S. W. Ødegård,<sup>7</sup> T. Page,<sup>1</sup> J. Pakarinen,<sup>2</sup> P. Reiter,<sup>8</sup> G. Sletten,<sup>9</sup> Ch. Theisen,<sup>5</sup> and H.-J. Wollersheim<sup>4</sup>



# The SAGE Spectrometer

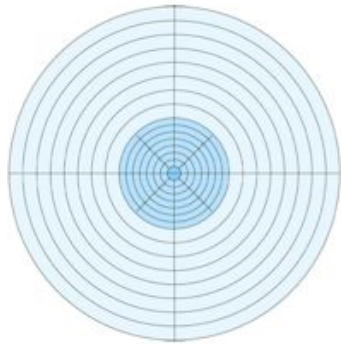


P. Papadakis et al., AIP Conf. Proc. **1090**, 14 (2009)

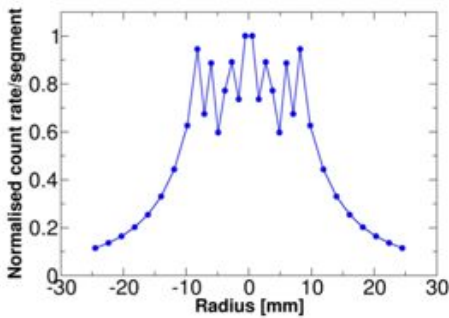


# SAGE - Silicon Detector

- 90 segments
- 51 mm diameter
- 1 mm thick



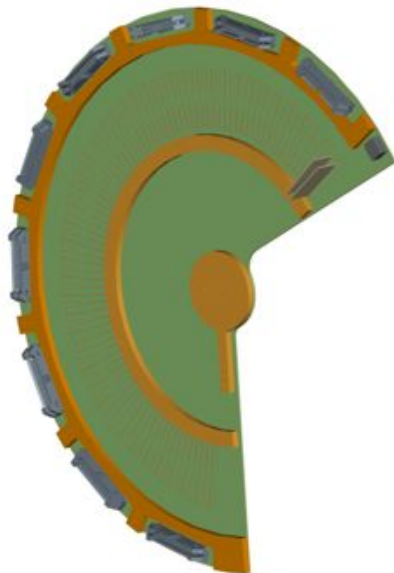
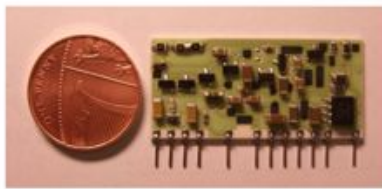
Simulated normalised count rate distribution  
using data from SACRED experiments



# SAGE - Silicon Detector

C.A.E.N. A1422 charge sensitive hybrid preamplifiers

- 400 mV/MeV
- Low noise
- Suitable for high count-rates



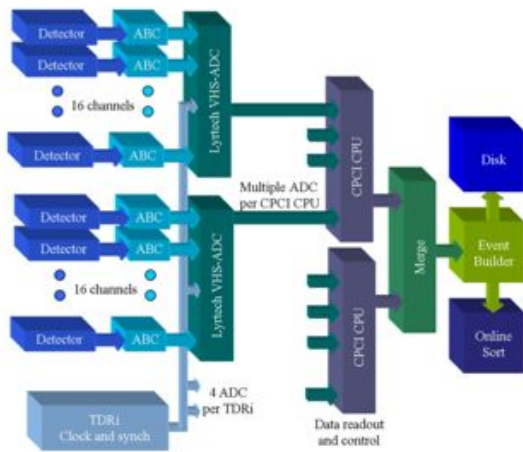
# SAGE - Electronics

201 Fully digital channels

90 Si channels

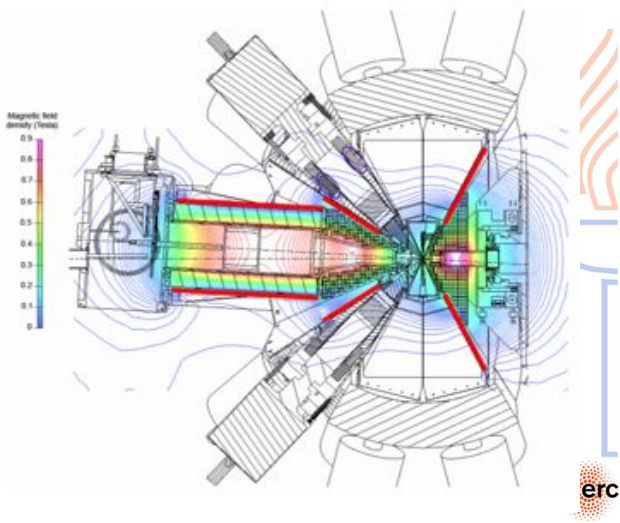
111 Ge channels

Lyrtech VHS-ADC



# SAGE - Shielding

- Photomultiplier tubes are sensitive to magnetic fields
- Shields: Weaken and redirect stray magnetic field



# The SAGE Spectrometer

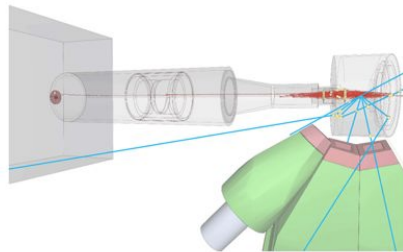
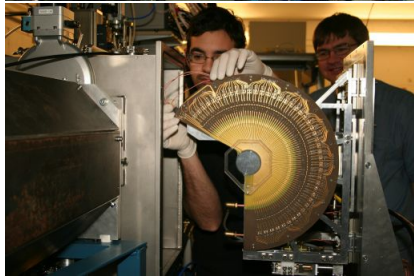


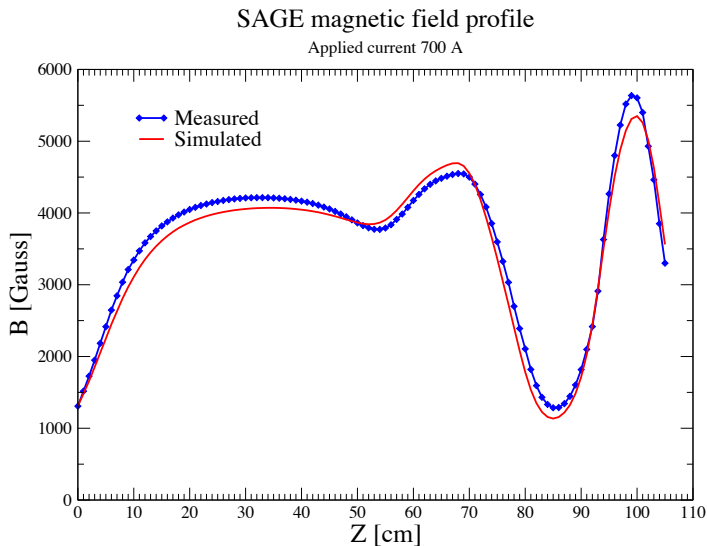
Figure 4.5: An example drawing of simulated events visualised in Geant4. Electrons are presented with red lines and gamma rays with blue. Only some of the electrons reach the detector while the others either interact with the surrounding materials (open circles) or are reflected back by the HV barrier. Note also the magnetic bottle effect of electrons being trapped in the magnetic field.

## Full Geant4 Simulation

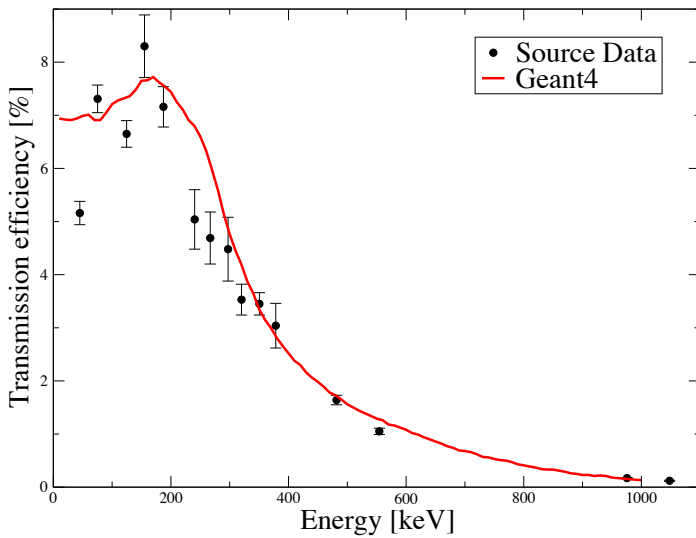
P.Papadakis, D.Cox, J.Konki, K.Hauschild, P. Rahkila



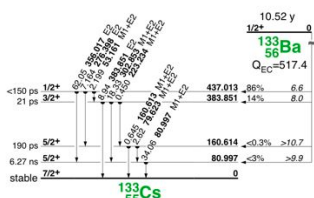
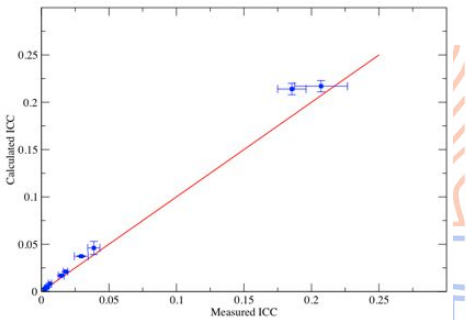
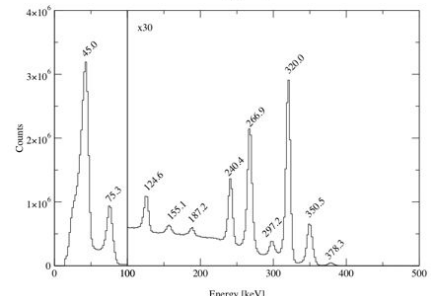
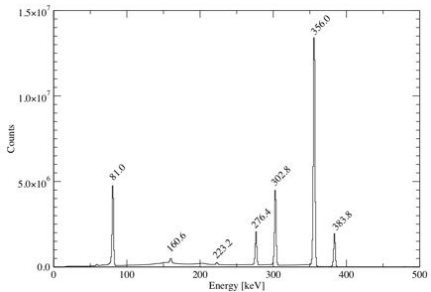
# SAGE - Field Profile



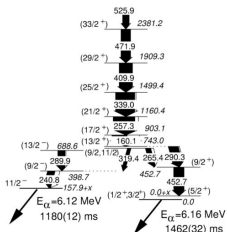
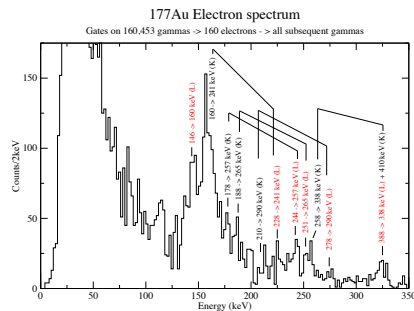
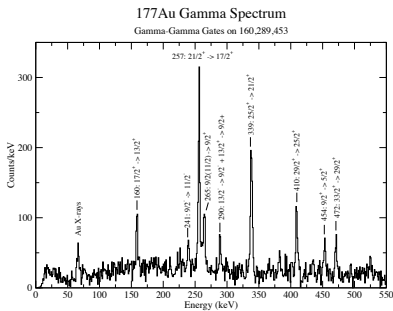
# SAGE- efficiency



# ICC determination with SAGE-<sup>133</sup>Ba



# ICC determination with SAGE-<sup>177</sup>Au Preliminary!



265 keV      9/2,11/2->9/2+ K:182.5keV      L:254keV		
ICC	Value	Error
K ICC Exp	0.132	0.037
K ICC BRICC	0.090	0.007
L ICC Exp	0.082	0.002
L ICC BRICC	0.050	0.001
K/L Exp	1.610	0.400
K/L BRICC	1.82	0.04

257 keV      21/2->17/2+ K: 176.5keV      L: 243keV		
ICC	Value	Error
K ICC Exp	0.088	0.024
K ICC Theo	0.091	0.004
L ICC Exp	0.062	0.014
L ICC BRICC	0.051	0.001
K/L Exp	1.421	0.508
K/L BRICC	1.644	0.04

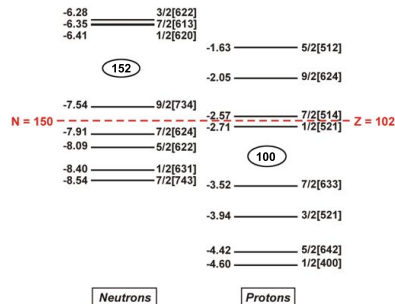
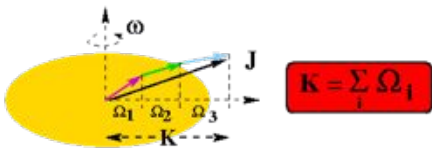
# Outline

- 1 Introduction
- 2 Experimental Approaches
- 3 Alpha Decay (Fine Structure) Spectroscopy
- 4 In-Beam Spectroscopy
- 5 Structure of High-K States
- 6 Future Perspectives



# K-Isomerism in $^{254}\text{No}$ and $^{250}\text{Fm}$

## The High-K state



- Transition forbidden if:  $\Delta K \leq L$
- Degree of forbiddenness  $\nu = \Delta K - L$
- Information on pairing gap,  $\Delta$  and single-particle energies,  $\epsilon_i$
- $E = \sqrt{(\epsilon_i - \lambda)^2 + \Delta^2} + \sqrt{(\epsilon_j - \lambda)^2 + \Delta^2}$
- Studies at focal plane - clean environment
- Often full decay path to ground state can be delineated

# K-Isomerism in $^{254}\text{No}$ and $^{250}\text{Fm}$

PHYSICAL REVIEW C

VOLUME 7, NUMBER 5

MAY 1973

## Isomeric States in $^{250}\text{Fm}$ and $^{254}\text{No}^\dagger$

Albert Ghiorso, Kari Eskola,\* Pirkko Eskola,\* and Matti Nurmiia

*Lawrence Berkeley Laboratory, University of California, Berkeley, California 94720*

(Received 30 November 1972)

- Isomeric states in  $^{254}\text{No}$  and  $^{250}\text{Fm}$  first postulated by Ghiorso et al., PRC7 (1973) 2032
- *The transfer of the  $^{250}\text{Fm}$  atoms from the wheel onto the movable detectors must then be caused by the feeble recoil resulting from the isomeric transition or other accompanying  $\gamma$  rays and conversion electrons in the cascade that leads to the ground state. For a 500 keV  $\gamma$  ray the recoil energy of a  $^{250}\text{Fm}$  atom is about 0.5 eV.*

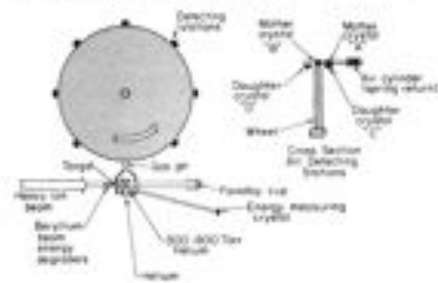
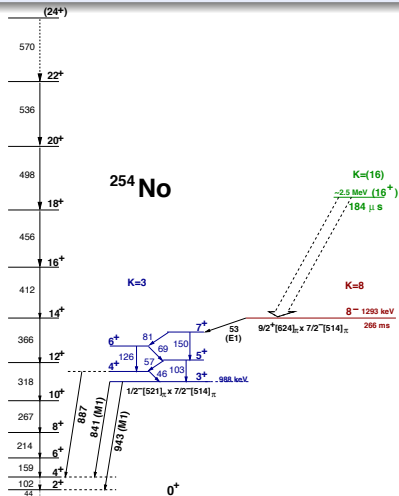


FIG. 1. A schematic diagram of the seven-detector-station system. The cross section at right shows the arrangement of the two movable mother detectors and the two stationary daughter detectors.

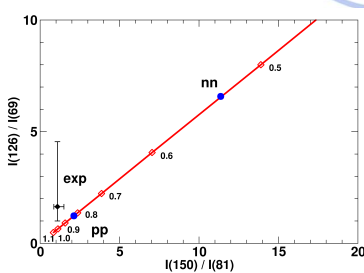
# K-Isomerism in $^{254}\text{No}$

R.-D. Herzberg et al., Nature **442**, 896-899 (2006)  
 S.K. Tandel et al., PRL **97**, 082502 (2006)

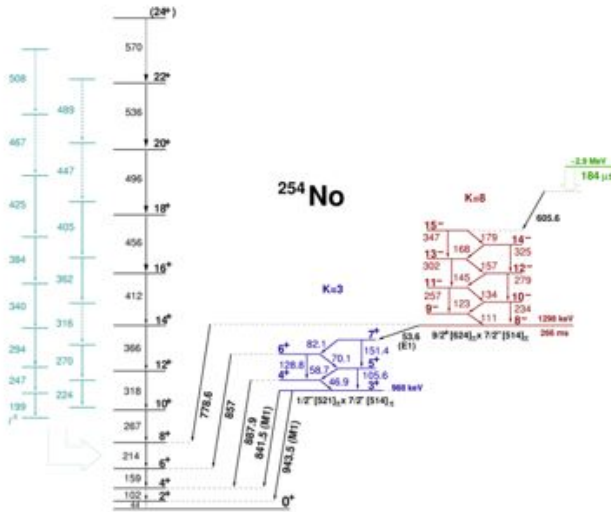


Determined Configurations:

$3^+ - (\pi[514]7/2^- \otimes \pi[521]1/2^-)$   
 $8^- - (\pi[514]7/2^- \otimes \pi[624]9/2^+)$   
 53keV E1  $\Delta K=5$ :  $f_\nu = 804$

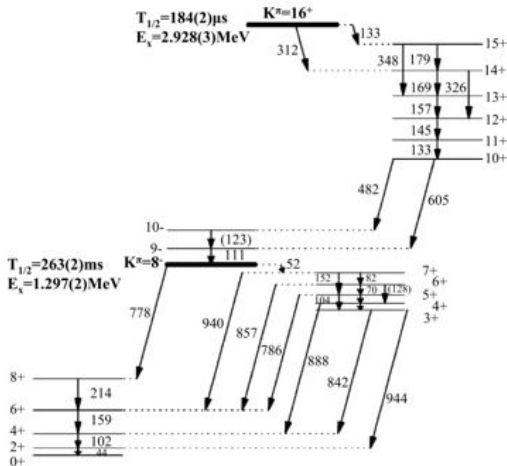


# K-Isomerism in $^{254}\text{No}$



F.P. Hessberger et al., EPJA **43**, 55 (2010) / C.Gray-Jones, Thesis, University of Liverpool

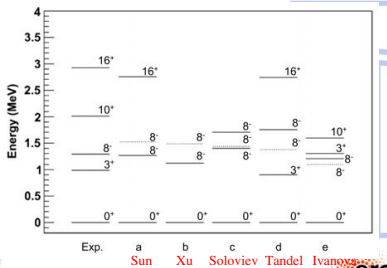
# K-Isomerism in $^{254}\text{No}$



R.M.Clark et al., PLB **690**, 19 (2010)

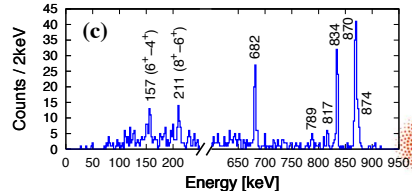
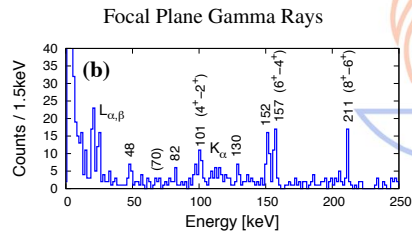
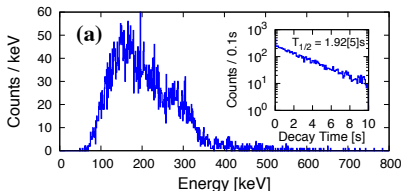
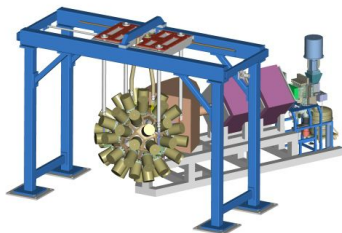
## Determined Configurations:

$3^+ - (\pi[514]7/2^- \otimes \pi[521]1/2^-)$   
 $8^- - (\nu[734]9/2^- \otimes \nu[624]7/2^+)$   
 or  $8^- - (\nu[734]9/2^- \otimes \nu[613]7/2^+)$   
 $10^+ - (\nu[734]9/2^- \otimes \nu[725]11/2^-)$   
 $16^+ - (\pi[514]7/2^- \otimes \pi[624]9/2^+) +$   
 $(\nu[734]9/2^- \otimes \nu[613]7/2^+)$



# K-Isomerism in $^{250}\text{Fm}$

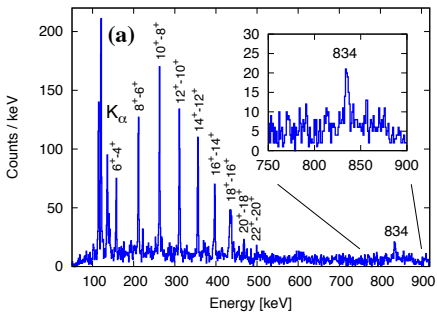
$^{48}\text{Ca} + ^{204}\text{HgS} \Rightarrow ^{250}\text{Fm} + 2\text{n}$ , JUROGAM+RITU+GREAT, P.T. Greenlees et al., PRC **78**, 021301(R) (2008)



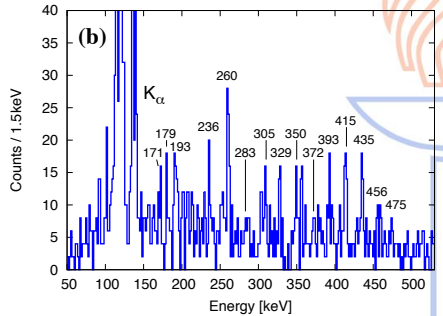
# K-Isomerism in $^{250}\text{Fm}$

$^{48}\text{Ca} + ^{204}\text{HgS} \Rightarrow ^{250}\text{Fm} + 2\text{n}$ , JUROGAM+RITU+GREAT, P.T. Greenlees et al., PRC **78**, 021301(R) (2008)

Ground State Band

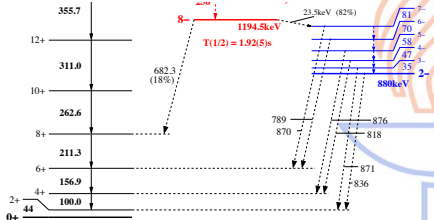
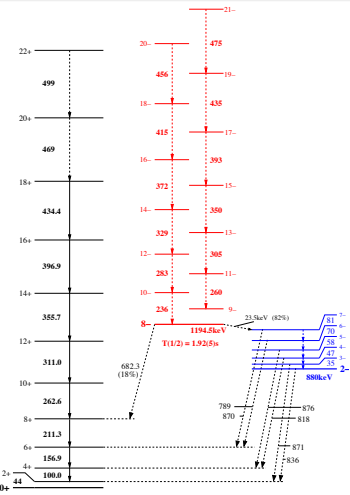


Isomer-Tagged Transitions



# K-Isomerism in $^{250}\text{Fm}$

$^{250}\text{Fm}$ : P.T. Greenlees et al. PRC **78**, 021301(R) (2008)



$8^- - \nu[624]7/2^+ \otimes \nu[734]9/2^-$   
 $2^- - \nu[622]5/2^+ \otimes \nu[734]9/2^-$  dominates  
 682 keV E1  $\Delta K=8$ :  $f_\nu = 213$   
 23.5 keV M1  $\Delta K=6$ :  $f_\nu = 192$

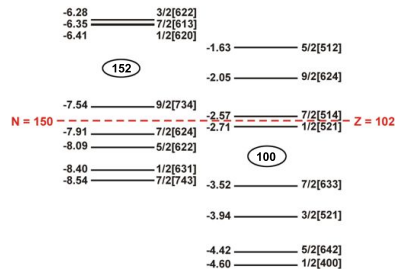
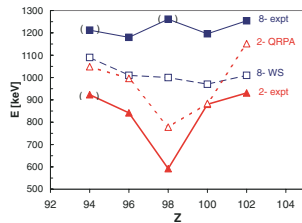
# Known 2QP K-Isomers in Region

Nucleus	$K^\pi$	$T_{1/2}$	$E_x$	Decay Mode	Configuration
$^{270}\text{Ds}$	$9^-, 10^-$	6 ms	$\simeq 1.13 \text{ MeV}$	$\alpha$	$9^- - \nu[725]11/2^- \otimes \nu[613]7/2^+$ $10^- - \nu[725]11/2^- \otimes \nu[615]9/2^+$
$^{256}\text{Rf}$	6,7?	$25 \mu\text{s}$	$\simeq 1.120 \text{ MeV}$	$\gamma$	??
$^{256}\text{Rf}$	10-12?	$17 \mu\text{s}$	$\simeq 1.400 \text{ MeV}$	$\gamma$	??
$^{254}\text{No}$	$8^-$	266 ms	1.293 MeV	$\gamma$	$8^- - \pi[514]7/2^- \otimes \pi[624]9/2^+$
$^{252}\text{No}$	$8^-$	110 ms	1.254 MeV	$\gamma$	$8^- - \nu[624]7/2^+ \otimes \nu[734]9/2^-$
$^{250}\text{No}$	$6^+?$	$42 \mu\text{s}$	??	SF, $\gamma$ ?	$6^+ - \nu[622]5/2^+ \otimes \nu[624]7/2^+$
$^{256}\text{Fm}$	$7^-$	70 ns	1.425 MeV	$\gamma, \text{SF}$	$7^- - \pi[633]7/2^+ \otimes \pi[514]7/2^-$
$^{250}\text{Fm}$	$8^-$	1.92 s	1.195 MeV	$\gamma$	$8^- - \nu[624]7/2^+ \otimes \nu[734]9/2^-$
$^{248}\text{Fm}$	??	$\simeq 8 \text{ ms}$	??	$\gamma$	??
$^{246}\text{Cm}$	$8^-$	??	1.179 MeV	$\gamma$	$8^- - \nu[624]7/2^+ \otimes \nu[734]9/2^-$
$^{244}\text{Cm}$	$6^+$	34 ms	1.040 MeV	$\gamma$	$6^+ - \nu[622]5/2^+ \otimes \nu[624]7/2^+$

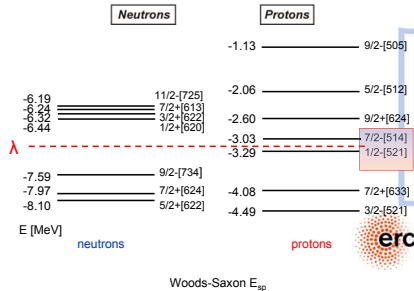
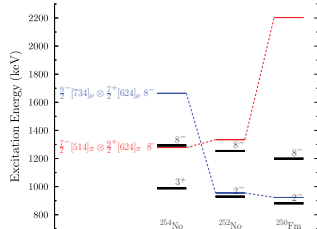
- References: See R.-D.Herzberg and P.T.Greenlees, Prog. Part. Nuc. Phys. 61, 674 (2008)
- $^{256}\text{Rf}$ : H.B.Jeppesen et al., PRC **79**, 031303(R) (2009)
- 3QP isomer in  $^{255}\text{Lr}$  (Dubna/GSI/JYFL/Berkeley). Also in  $^{253}\text{No}$

# Systematics of 2 quasi-particle states

N=150: A.Robinson et al., PRC **78**, 034308 (2008)



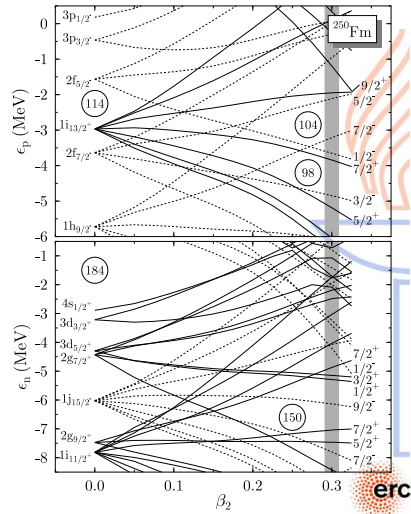
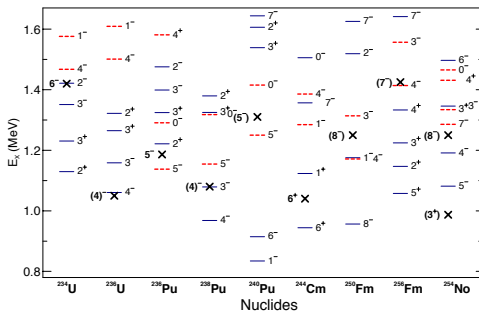
N=150/152: P.T.Greenlees et al., PRC **78**, 021303(R) (2008)



# Self-Consistent Calculations

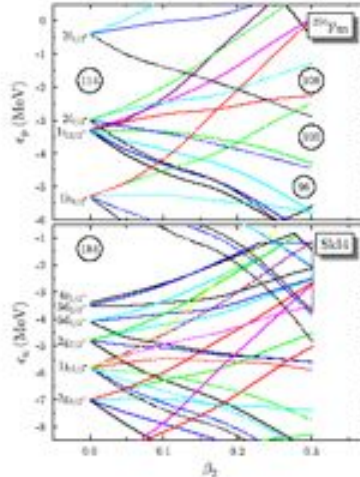
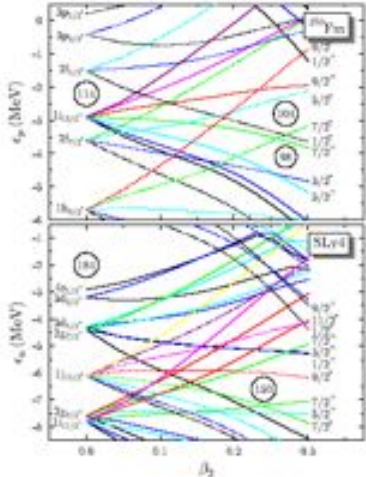
HFB SLy4 - from A.Chatillon et al., EPJA **30** 397 (2002)

HFB Gogny D1S  
J.-P. Delaroche et al., Nucl. Phys. **A771**, 103 (2006)



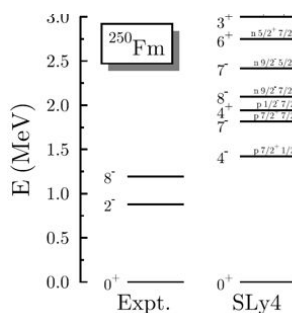
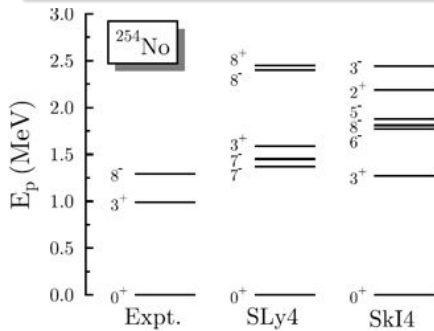
# Self-Consistent Calculations

Taken from Talk of Paul-Henri Heenen (<http://nuclear1.paisley.ac.uk/SHEworkshop/>)



# Self-Consistent Calculations

Taken from Talk of Paul-Henri Heenen (<http://nuclear1.paisley.ac.uk/SHEworkshop/>)



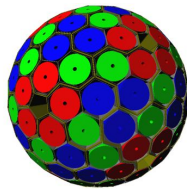
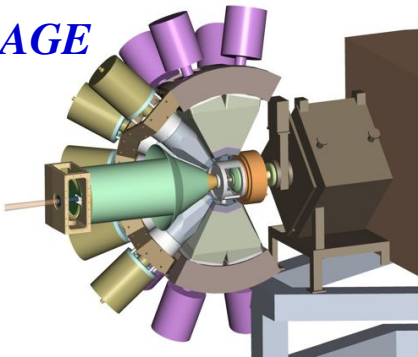
# Outline

- 1 Introduction
- 2 Experimental Approaches
- 3 Alpha Decay (Fine Structure) Spectroscopy
- 4 In-Beam Spectroscopy
- 5 Structure of High-K States
- 6 Future Perspectives



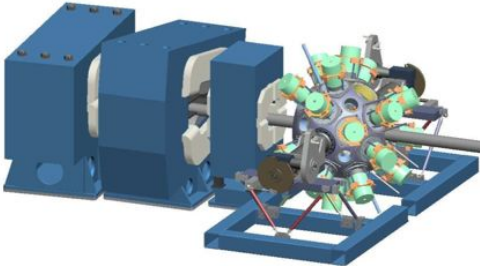
# In-beam spectroscopy: Future

**SAGE**

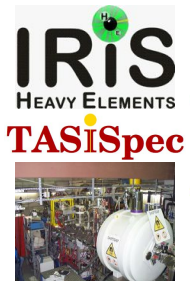


Paul Greenlees (JYFL, Finland)

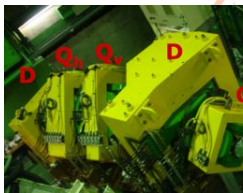
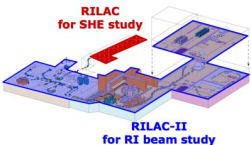
Spectroscopy of VHE



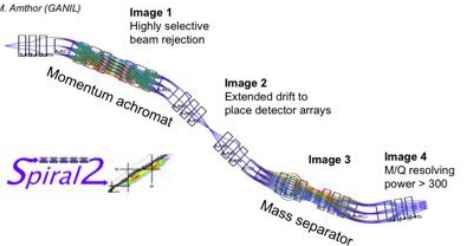
# Future with Stable Beams: Upgrades / New Devices



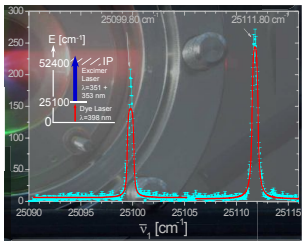
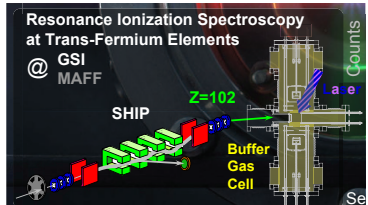
## SHE study in RIBF (After 2011)



M. Amthor (GANIL)



# Optical spectroscopy of heaviest elements



- Sample of  $^{255}\text{Fm}$  produced at ORNL
- Breeding of  $^{255}\text{Es}$  from  $^{246}\text{Cm}$
- Sample transported to Germany (about  $10^{11}$  atoms)
- Two-step RIS, Fm confirmed with QMS
- Determined location of atomic levels for first time
- Heavily dependent on atomic theory

M. Sewtz et al., PRL **90**, 163002 (2003)

Paul Greenlees (JYFL, Finland)

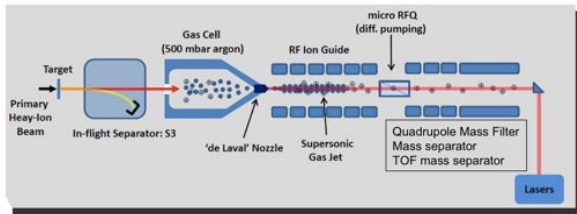
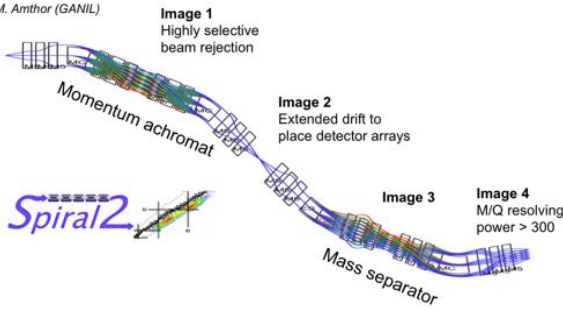
Spectroscopy of VHE

EJC2012

69 / 77

# Optical spectroscopy of heaviest elements

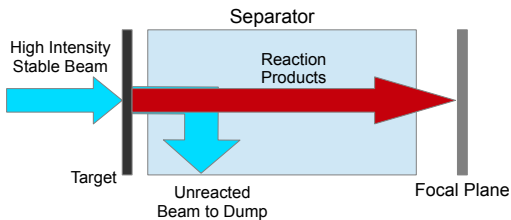
M. Amthor (GANIL)



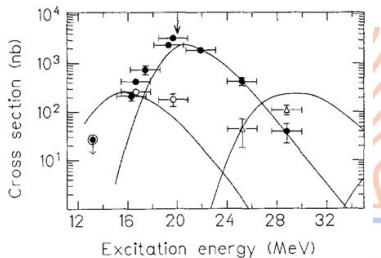
P.Van Duppen et al., LoI for SPIRAL2



# Production of heavy radioactive "beams"

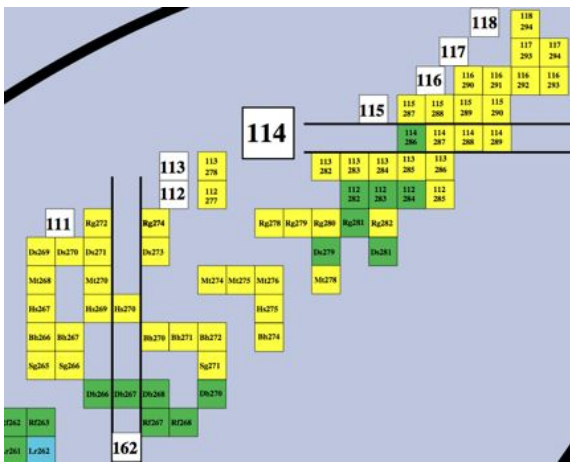


- Typical separator efficiency 50%
- Primary beam suppression e.g.  $10^{12}$
- 10 p $\mu$ A beam  $^{48}\text{Ca}$
- 0.5 mg/cm $^2$   $^{208}\text{Pb}$  target
- $\rightarrow 150\text{pps } ^{254}\text{No}$



- Only one reaction product
- Narrow excitation function (10 MeV in lab)
- No increase in yield with thick target
- Energy  $\simeq 0.2 \text{ MeV/u}$
- Could use inverse kinematics

# Possibilities with RIBs



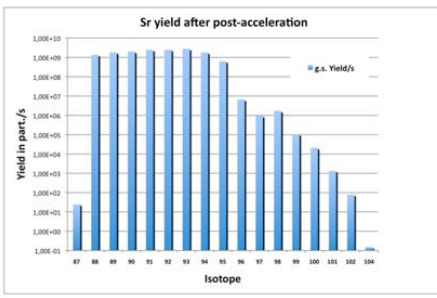
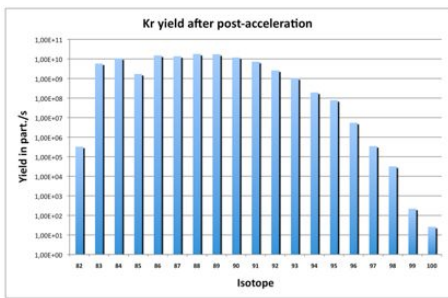
## Around N=152/162

- $^{90-94}\text{Kr} + ^{164}\text{Dy} \rightarrow ^{254-258}\text{No}^*$
- $^{90-94}\text{Kr} + ^{160}\text{Gd} \rightarrow ^{250-254}\text{Fm}^*$
- $^{132}\text{Sn} + ^{137}\text{Cs} \rightarrow ^{267}\text{Db}^*$
- $^{132}\text{Sn} + ^{132,134,136}\text{Xe} \rightarrow ^{264,266,268}\text{Rf}^*$
- $^{132}\text{Sn} + ^{138}\text{Ba} \rightarrow ^{270}\text{Sg}^*$
- $^{132}\text{Sn} + ^{139}\text{La} \rightarrow ^{271}\text{Bh}^*$
- $^{132}\text{Sn} + ^{140,142}\text{Ce} \rightarrow ^{272,274}\text{Hs}^*$
- $^{132}\text{Sn} + ^{142-150}\text{Nd} \rightarrow ^{274-282}\text{Ds}^*$
- $^{90-96}\text{Kr} + ^{181}\text{Ta} \rightarrow ^{271-277}\text{Mt}^*$
- $^{90-96}\text{Kr} + ^{186}\text{W} \rightarrow ^{276-282}\text{Ds}^*$
- $^{90-96}\text{Kr} + ^{180}\text{Hf} \rightarrow ^{270-276}\text{Hs}^*$
- $^{90-96}\text{Kr} + ^{175,176}\text{Lu} \rightarrow ^{265-272}\text{Bh}^*$
- $^{90-96}\text{Kr} + ^{176}\text{Yb} \rightarrow ^{266-272}\text{Sg}^*$

## Towards N=184?

- Difficult even with radioactive beams
- $^{90-95}\text{Kr} + ^{208}\text{Pb} \rightarrow ^{298-303}118^*$
- $^{132}\text{Sn} + ^{170}\text{Er} \rightarrow ^{302}118^*$
- $^{132}\text{Sn} + ^{176}\text{Yb} \rightarrow ^{308}120^*$

# SPIRAL2 Predicted Intensities



- Figures assume  $5 \times 10^{13}$  fissions/sec
- Phase2 Day1, 50 kW d beam: e.g.  $^{92}\text{Kr}$   
 $6.2\text{MeV/u } 2.6 \times 10^8 \text{ pps}$



# EURISOL Predicted Intensities

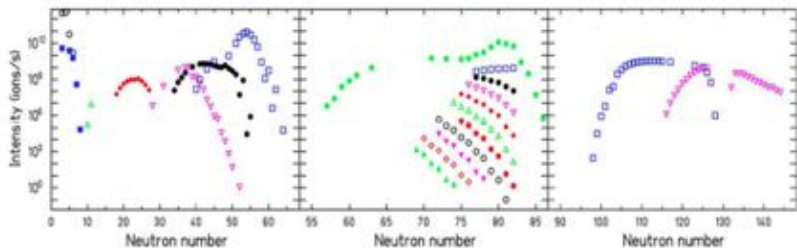


*Fig. 13: Predicted EURISOL intensities of several nuclides:*

Left: Be (black open dots),  
Li (blue filled squares),  
Mg (open green triangles),  
Ar (red filled rhomboids),  
Ni (magenta open triangles),  
Ga (black filled dots),  
Kr (open blue squares);

Centre: Zr (filled green triangles),  
Nb (open red diamonds),  
Mo (magenta filled triangles),  
Tc (black open dots),  
Ru (red filled dots)  
Rh (green open triangles),  
Pd (red filled diamonds)  
Ag (magenta open triangles)  
Cd (filled black dots),

Right: Hg (squares)  
Fr (triangles)

# Possibilities with RIBs

## Atomic Physics and Chemistry of the Transactinides

> 5 atom/day list

- >  $^{264}\text{Rf}$        $^{252}\text{Cf}(^{16}\text{C}, 4n)$
- >  $^{265}\text{Db}$        $^{249}\text{Bk}(^{20}\text{O}, 4n)$
- >  $^{268}\text{Sg}$        $^{252}\text{Cf}(^{20}\text{O}, 4n)$
- >  $^{267}\text{Bh}$        $^{252}\text{Cf}(^{21}\text{F}, 6n)$

W. Loveland, FUSHE2012

See also W.Loveland PRC **76** 014612 (2007)

N.B. Does not include detection efficiency

What kind of reactions with RNBs are used to form n-rich nuclei?

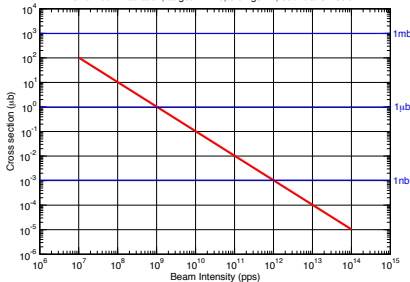
Reactants	Products	FRIB Beam Intensity (p/s)	Production Rate (atoms/day)
$^{26}\text{Ne} + ^{248}\text{Cm}$	$^{271}\text{Sg} + 4n$	$2.2 \times 10^6$	0.004
$^{30}\text{Mg} + ^{244}\text{Pu}$	$^{270}\text{Sg} + 4n$	$7.1 \times 10^6$	1
$^{29}\text{Mg} + ^{244}\text{Pu}$	$^{269}\text{Sg} + 4n$	$3.6 \times 10^7$	0.2
$^{20}\text{O} + ^{252}\text{Cf}$	$^{268}\text{Sg} + 4n$	$1.5 \times 10^8$	5
$^{23}\text{Ne} + ^{248}\text{Cm}$	$^{267}\text{Sg} + 4n$	$1.6 \times 10^8$	1



# The Limits

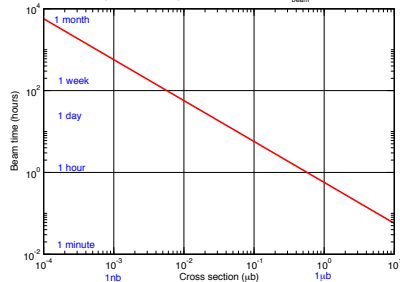
## Minimum requirement for in-beam studies

Cross section required to accumulate 300 full-energy alpha decays  
One week irradiation, target A=170,  $0.5\text{mgcm}^{-2}$ , 50% transmission



## Minimum requirement for decay/reaction mechanism studies

Beam time required to accumulate 10 full-energy alpha decays  
Target A=170,  $0.5\text{mgcm}^{-2}$ , 50% transmission,  $I_{beam}=10^{10}$  pps



$$10^{12} \text{ pps}, \text{XS } 1\text{pb} \rightarrow 0.3 \text{ events/week}$$

# Summary

- Detailed spectroscopy of heavy elements can provide high quality data and level assignments
- In-beam spectroscopy at 10 nb level
- Decay spectroscopy at sub-nb level
- Data is providing challenges for theory
- Hopefully will lead to a better understanding of the structure of SHE
- Laser and Mass Measurements will bring much-needed new information
- Many new facilities being built and upgrades going on
- Some opportunities to produce new isotopes from secondary reactions with RIBs
- Still much to be done (for both experiment and theory)

